Chapter 3

Photonic Band Gap of Two-dimensional Photonic Crystals with Broken Structural and Rotational Symmetries

For two dimensional photonic crystals, the electromagnetic waves in the complete PBG can not propagate in two dimensions, and may be able to propagate in other direction. The width of complete PBG at least larger than ***kT*** is required for device applications. If we consider the energy ***E*** located at the centre of a large band gap, the photons with energy ***E*** in in-plane propagation can be controlled well and its extent of incident angle can be increase. Since the photonic devices for the applications always operate at a fixed energy or a fixed energy range, it is preferable to have a large band gap at a higher normalized energy. The gap center located at high frequency means that the lattice constant of photonic crystal is large, and the photonic device may be fabricated easily. Recently, Many attempts have been made to design various kinds of photonic band structures in an effort to obtain a large PBG, such as choosing materials and structures, inserting a third component into system and reducing the structural symmetries.[33,38-41,51,52]

There are two main approaches for obtaining large complete PBGs. One approach is to augment the gap width of the E-polarization or H-polarization modes, and the other approach is to enlarge the overlap of both polarization modes.[41] Note the E-polarization and H-polarization modes are the electric and magnetic fields polarized along the rod axis respectively. With regard to the first approach, the most

severe limit to the PBG width is due to the degeneracy of photonic bands at high symmetry points in the Brillouin zone. Several methods have been suggested for lifting the band degeneracy and obtaining the complete PBG, which involve varying the contrast of dielectric contrast ratio, lattice structure and filling ratio. The dielectric contrast ratio is often limited by material properties and causes a severe constraint to the search for photonic crystal with large complete PBGs, particularly in the technologically important near-infrared region. Several groups have introduced metallodielectric materials with large dielectric constant into the photonic crystals; however, these materials also suffer from absorption.[53]

The symmetry of photonic crystal plays a very important role in enlarging the PBGs. The symmetry-breaking patterns can change the aspect of the dispersion curves, either by opening some additional gaps or by widening the existing gaps. There are two familiar methods to reduce the symmetries of photonic-crystal band structures. One is to insert a different size rod or a third component into the original structure to reduce its structural symmetry. For example, in square lattice and honeycomb structure, and in group 4mm photonic crystals, small circular rods are inserted between the original circular rods; the degeneracy bands are split and consequently the PBG widths are widened.[35,39,54] Anderson and Giapis have shown in 2D photonic crystal that the gap width for either E-polarization or H-polarization modes and the overlap for both modes can be increased by inserting a different rod into the square lattice.[35] The results shown some gaps at high frequency region is enlarged, the ones at low frequency region is often reduced as the symmetry is broken.

The other method to reduce the structural symmetry of photonic crystal is through the use of irregular lattice or rod into the structure. Several dielectric functions of regular rods have been shown in the chapter two. In particular, the circular rod exhibits

full symmetries, including rotation, inversion, and translation symmetries. The inversion and rotation symmetries will be broken as the rods are deformed to oval rods. Early studies on triangular lattice with oval, square, rectangular and hexagonal rods fail to open new gaps or create larger gaps than those using circular rods.[36-38] The use of the circular rods in triangular lattice is the best design to obtain the largest complete PBGs. More recently, It has also been reported that the complete PBGs of 2D photonic crystals can be widened not only by deforming the shape of rods but also by rotating the orientation of rods, which are usually designed in triangular, square and hexagonal lattice with various shapes and cross sections.[29,55-57] The degenerate band structures at high-symmetry points in the first Brillouin zone can be split, and even cause both polarization modes to overlap each other by reducing the rotational and structural symmetries.

In this chapter, we systematically investigate how the effect of reduction of symmetry on the photonic band structure. The two-dimensional triangular and square photonic crystals are considered. The optimal parameters in obtaining the largest PBG are calculated and the parameters influencing the formed PBG are examined. Moreover, the effect of structural and rotational symmetries associated with the deformation and rotation of rods on E-polarization and H-polarization band gaps has also been studied. We choose the media with dielectric constant $\varepsilon = 12.96$ (gallium arsenide or silicon at $1.55\ \mu\mathrm{m}$) and air with dielectric constant $\varepsilon = 1$ as inclusions in the photonic crystal. The air/GaAs patterns of submicron size can be made by reaction ion etching (RIE). The plane-wave expansion method is used for calculations of photonic band structures. We use 625 plane waves throughout the calculations of this chapter. The convergence accuracy for the lowest twenty photonic bands of both E- and H-polarization modes is better than 1%.

3.1. Air Rods with Triangular Lattice

It is well known that the triangular lattice embedded with circular air rods can create an complete PBG. Figure 3.1 displays the band structure of a photonic crystal consisting of circular air rods at a filling factor $f = 0.8$. The solid curves are for the E-polarization modes and the dotted curves are for the H-polarization modes. The dispersion curves have been traced along the T-M-K-T path in the first Brillouin zone. Three high-symmetry points T, M, and K correspond to $\vec{k}_{\|} = 0$, $\vec{k}_{\|} = \frac{2\pi}{a}(\frac{1}{2}\hat{e}_x - \frac{1}{2\sqrt{3}}\hat{e}_y)$ and $\vec{k}_{\|} = \frac{2\pi}{a}(\frac{2}{3}\hat{e}_x)$. The inset in figure shows the high-symmetry points at the corner of the irreducible Brillouin zone (shaded region). The shading region in the figure represents the complete PBG, which the light can not propagate in this frequency region.

The appearance of complete PBG in this photonic structure is attributed to the arrangements of connected dielectric veins and isolated dielectric spots. The schematic drawing of vein and spot in the triangular lattice is displayed in Fig. 3.2. From the rule of thumb, the isolated high-dielectric spots are favorable for the large E-polarization band gaps, while the connected veins are favorable for the large H-polarization band gaps.[43] So an complete PBG is favored in photonic crystals with high-dielectric regions that are both practically isolated and connected.

Figure 3.3 displays the gap map plotted with respect to the filling factor f. As the results, the bands for both E-polarization and H-polarization modes move toward high frequencies when the filling factor increases. The band-structure features can be understood easily by considering the average dielectric constant. The increase in the filling factor leads to the decrease in the value of average dielectric constant of the photonic crystal. This indicates that the field-energy proportion concentrated in the dielectric region is reduced, resulting in the increase of normalized frequency of band.

Therefore, the overall photonic dispersion curves for either E- or H-polarization modes tend to move toward high frequency. We also see that E-polarization gaps can not open until the filling factor is great than 0.6. The absence of E-polarization gap for small filling ratio may be supposed that the field energy in the dielectric-spot regions can not appear a large difference between dielectric and air bands. To understand how the field distribution dependent on the filling factor, the field patterns of the two lowest E-polarization bands are calculated. Figures 3.4(a)-(d) show the level distribution of the displacement field for $f = 0.3$ and $f = 0.85$ in the two lowest bands. Each figure plots the displacement-field distributions associated with the first and second bands at the T-symmetry point. As the diagrams indicate, the difference in field distributions between 1st and 2nd bands for $f = 0.3$ is smaller than that for $f = 0.85$. The similar field patterns for dielectric and air bands imply that the dielectric-band frequency approaches to the air-band frequency, resulting in the absence of E0polarization gap. Moreover, the thumb rule has shown that the isolated spots favor in the appearance of the E-polarization gap. In comparison with the description in Fig. 3.2, we find the photonic structure with $f = 0.85$ has constructed the isolated dielectric spots in the field patterns. The large difference in field distribution between dielectric and air bands and the formed isolated spots may cause the appearance of E-polarization gap at large filling factor. For the H-polarization mode, the gap widths are increased when the filling factor is increased. Because the H-polarization fields are oriented in the x-y plane, the partial tangential fields that link nearest-dielectric veins must be forced to penetrate regions of air to satisfy the continuity boundary condition. For this reason, the variation in the interaction between high-dielectric veins strongly influences the fraction of field energy in the dielectric regions, and thereby enlarges the H-polarization gap width.

The maximum width of complete PBG is obtained when the filling factor is

designed with 0.85. This structure possesses both isolated dielectric regions and connectivity and is the almost close-packing condition for circular rods in the triangular lattice. Since the maximum filling factor for the triangular lattice with circular rod is $f = 0.91$, the dielectric size between air circular rods is very thin for $f = 0.85$. Therefore, the photonic structure for application is difficult to fabricate. Generally, one would expect the complete PBG to get larger as the filling factor is increased. In fact, since the E-polarization and H-polarization modes in 2D photonic crystal are decoupled and are dominated by different equations. The enlargement and overlap do not follow a simple rule and may be optimized by the proper design of structure, filling factor and material.

Next, we replaced full-symmetry circular rods with square rods in the triangular lattice to study the formation of PBG. Note the parameters in calculations are the same with that in circular case. The frequencies calculated along symmetry directions of first Brillouin zone are plotted in Fig. 3.5. The H-polarization gap of square rods with triangular lattice resembles to that of circular rods, but there are some novel E-polarization gaps appearing in the square rods. The reason why the E-polarization bands are split is that the symmetry of photonic crystal may be changed by the use of square rods. It is supposed that the variations in field distribution inside the dielectric region lead to alter the E-polarization band. The difference in band structures between circular and square rods will be calculated and examined systematically in chapter 4.

Figure 3.6 plots the gap map as a function of filling factor associated with the square rods of triangular lattice. The first thing we notice is that there are two complete PBGs in this structure, which are labeled G1 and G2 in figure. The features of band structure on increasing filling factor can also be understood by using the same qualitative arguments as that for circular rods. In particular, we see that numerous E-polarization band gaps are observed for this 2D photonic crystal, and the

E-polarization gap can be opened at small filling factor. The complete PBG G1 opens at a smaller filling factor $f = 0.55$ and closes at $f = 0.8$; the G2 opens at $f = 0.65$ and reaches the maximum gap width at $f = 0.85$. Comparing with the previous results of circular rods, the width of complete PBG for the present PC consisting of square rods is smaller. In Fig. 3.7 the gap width to mid-gap frequency ratio is plotted with respect to the filling factor for the complete PBG as shown in Figs. 3.1 and 3.6. The maximum width of complete PBG is for the circular rods at $f = 0.85$, approximately 2 times larger than the maximum gap width for the square rods. The results show that full-symmetry circular rods with triangular lattice can overlap both modes well at high filling factor, while the square rods with triangular lattice can open more E-polarization gaps.

3.2. Dielectric Rods with Square Lattice

The use of circular rods is a well design to obtain the larger complete PBG than the use of square rods in triangular lattice. In particular, only the air rods with triangular lattice can overlap both polarization modes and appear complete PBGs. The dielectric rods with triangular lattice can not appear an overlap of both polarization modes; this point will be examined further in the following section. For the photonic structure based with square lattice, the large complete PBGs appear when the rods are designed as dielectric media and almost close when the rods are designed in air. This condition is contrary to the case based with triangular lattice. In this section, we turn to examine the formation of PBG by using square lattice in the photonic structure.

Figures 3.8(a) and (b) show the photonic band structures associated with circular and square dielectric rods embedded with square lattice, respectively,

at the filling factor of 0.45. The inset in figure shows the high-symmetry points at the corner of the irreducible Brillouin zone (shaded region). The dispersion curves have been traced along the T-X-M-T path in the first Brillouin zone. Three high-symmetry points T, X, and M correspond to $\vec{k}_{\|}=0$, $\vec{k}_{\|}=\frac{2\pi}{a}(\frac{1}{2}\hat{e}_x)$ and $\vec{k}_{\|}=\frac{2\pi}{a}(\frac{1}{2}\hat{e}_x-\frac{1}{2}\hat{e}_y)$. As shown in Fig. 3.7(a), the circular rods with square lattice can not open an enough size of H-polarization band gap when the frequency is less than $1.0\ (\omega a/(2\pi c))$. Therefore, the results shown the circular dielectric rods with square lattice can not open the complete PBG. The isolated columns may favor to open E-polarization band gap, but this structure lack for dielectric veins to open H-polarization band gap. On the contrary, the band structures of square rods in the square lattice are shown in Fig. 3.7(b), with a sizable complete PBG at higher frequencies of EM waves. The complete PBG occurs where E_8 and H_6 gaps overlap, where E_i and H_i denote the gap that appears between the ***i***th and (***i***+1)th bands for the corresponding polarization.

It is interesting that the isolated-dielectric rods can appear an complete PBG by the use of square rod without including dielectric veins. The band structures of square lattice of circular and square dielectric rods in air have been reported.[36,58] However, very few attempts have been made at such observation. This problem will be calculated and investigated from the perspective of polygonal and edge-cutting structures in the next chapter. The influence of polygonal columns on the corresponding dispersion curves and field distributions will be studied there. Following we only limit our discussions to the effect of filling factor on the band structures of dielectric rods with square lattice.

Figure 3.9(a) shows the gap map for the square lattice of circular dielectric rods as a function of filling factor. Here we only consider the bands below fourteenth band for both polarizations. The width of H-polarization gap can not be widened by increasing filling factor, resulting in the absence of complete PBG. Moreover, gap widths in this photonic crystal are closed at large filling factor. The gap map for square lattice of square dielectric rods as a function of filling factor is displayed in Fig. 3.9(b). The complete PBG ranges from $f = 0.25$ (d/a=0.5) to $f = 0.65$ (d/a=0.81), where d is the size of side of square rod. This photonic crystal has the maximum width of complete PBG at $f = 0.4$, which corresponds to d/a=0.63. H_6 is the only H-polarization gap appearing below the fourteenth band. Therefore, this photonic crystal has the only one complete PBG throughout the filling factors.

For the triangular lattice the complete PBG exists in the case of air columns, and reaches maximum for the circular cross section of the columns. For the square lattice the complete PBG exists in the case of dielectric columns, and reaches maximum for the square cross section of the columns. In particular, the square lattice of circular dielectric rods can not open complete PBG by changing filling factor. The results show that the largest width of complete PBG appears when the shape of rods resembles the shape of Brillouin zone.

Since the PBG should be open in all directions, early studies have indicated that the circular Brillouin zone is preferable to widen the gap widths and the three dimensional structures with circular Brillouin zone are employed in obtaining large PBG.[32,59,60] Normally, the PBG for the triangular lattice is larger than that for the square lattice whose Brillouin zone is square shaped. Furthermore, the lattice structure and the shape of rods play very important

roles in opening and getting the large complete photonic band gaps. The largest complete PBG is achieved as the lattice symmetries are the same with the columns' symmetries; such as the circular rods in triangular lattice and square rods in square lattice. More photonic crystals consisting of lattices with different symmetries and columns of various shapes have been studied.[61,62] Accordingly, the investigation in structural symmetries of photonic crystals is important for understanding the formation of PBGs and may provide design routes for desired PBGs.

3.3. Effects of Deformed and Rotational Symmetries on Band Structures

We have shown that the isolated dielectric regions favor the E-polarization band gap, and the connected dielectric regions favor the H-polarization band gap. So an complete PBG is favored in photonic crystals with high-dielectric regions that are both practically isolated and connected. Following these ideas, the large complete PBGs have been obtained through adjusting the filling factors of regular rods. Our calculations in section 3.1 have shown that the complete PBGs often appear at a larger filling factor, the results indicate these structures are difficult to fabricate with too thin veins. Thus, it is important to choose in priority the one with a filling factor far less than the close-packing one from different photonic structure possessing the equal size of complete PBG. Two-dimensional lattices with irregular rods may be the promising candidates to be freely adjusted the isolated dielectric regions and connected veins by deforming and rotating the rods. In this section, we expand these ideas to widen the complete PBG width by using deformed and rotational rods.

The effects of deformed and rotational symmetries on the band structures have been studied.

For simplicity and not without generality, we prefer to focus on the 2D triangular lattice of the air rods in a dielectric background. The parameters are the same with the case in section 3.1, and the schematic diagram and representation of rods in the triangular lattice are shown in Fig. 3.9. $\bar{a}_1$ and $\bar{a}_2$ are the basic vectors of the triangular lattice. The lattice constants are defined as $a = |\bar{a}_1| = |\bar{a}_2|$. The cross-sectional area of the triangular lattice is given by $A_{cell} = |\bar{a}_1 \times \bar{a}_2|$. The dimensions of the rods along the major and minor axes are given by (a_x, b_y) in units of the lattice constant. For convenience, the ratio of the dimensions along the major and minor axes for the oval rods is denoted $\alpha = a_x / b_y$. The θ represents a rotating angle with respect to the x axis. In this work, we investigate how rotational and structural symmetries affect the E- and H-polarization modes of circular rods embedded with triangular lattice. Moreover, the optimal parameters associated with the large PBG for this photonic crystal will be determined.

In the beginning, we examine the variations in complete PBG width by varying the shape of rods. The y-axis size b_y of oval rod is kept constant, and ratio α is varied solely by a_x. In fact, the significant deviations for the etching process of circular rods in the 2D photonic crystal have been reported. Accordingly, the presented design for calculations can also be helpful to understand the effects of deteriorating structure roundness on the band structures.

Figure 3.11 shows the normalized gap width of complete PBG as a

function of b_y for various α. The geometric parameters of the rods of each structure are designed to not overlap with the nearest neighboring rods under deformation. When b_y is less than 0.48, the complete PBG width of full-symmetry circular rods is larger than those of deformed structures, and the circular rod with radius of $b_y = 0.48\,a$ has the maximum complete PBG width in the triangular lattice. For a given value of b_y, the decrease of ratio α indicates the filling factor of column is decreased. Thus, the decrease of gap widths for deformed structures is due to the decrease of filling factors. Now we turn to plot the gap map at $\alpha = 0.75$, $\alpha = 0.85$ and $\alpha = 0.95$, as shown figures 3.12(a)-(c) respectively, to examine how the deformed rods affect the band gaps of both polarizations. Here we replace b_y with filling factor in Fig. 3.12. It is observable that band gaps for both polarizations are almost the same with those in Fig. 3.3. Thus, the triangular lattice coupled with noncircular rods fails to open new complete PBG or create PBGs larger than those using circular rods. The filling factor mainly determines the formation of PBG of air rod in triangular lattice even though the rods are deformed.

Next, we consider not only the deformation but also the rotation of rods to affect the photonic band structures in the triangular lattice. Only the filling factors $f = 0.6,\ 0.65$ and 0.7 are chosen and to not overlap with the nearest neighboring rods under deformation and rotation. Figure 3.13 displays the dependence of normalized complete gap width on f for various α through a rotation angle of $\theta = 30^\circ$. The results reveal that the photonic structure of $\alpha = 0.8$ at $\theta = 30^\circ$ obtains the maximum complete PBG width throughout the calculations. The increase of the gap width, observable for $\alpha < 1$ in figure, is a

combined effect of the deformation and rotation of rods. The gap maps at $\alpha = 0.8$ and $\alpha = 0.9$ through a rotation angle of $\theta = 30^\circ$ are plotted in Figs. 3.14 (a) and (b), respectively. In comparison with Figs. 3.12 and 3.3, it is obvious that more H-polarization gaps are opened and widened when the rods are rotated. For the noncircular rods, the dielectric regions between the neighboring air rods are changing by rotating rods. The electromagnetic interactions between dielectric regions are varied strongly, and thereby enlarge the H-polarization gap width. Accordingly, the reason why the complete PBG width can be widened in rotational structures can be understood. Through adjusting the filling factor and the rotation angle, the E-polarization band gap may overlap with the H-polarization band gap; consequently, a large complete PBG will be obtained.

3.4. Effect of Anisotropic Materials on Band Structures

In above sections, we have shown that the structures of air rods in the triangular lattice can create complete PBGs. However, our calculations have also shown that the use of dielectric circular or square rods as inclusions in the triangular lattice can not open the complete PBG. Figs. 3.15(a) and (b) show the gap maps plotted with respect to the filling factor and refractive index for dielectric circular rods in the triangular lattice, respectively. The filling factor of rods is fixed as $f = 0.45$ for the calculations in Fig. 3.15(b). The band-structure features for two cases can also be understood by using the same qualitative arguments as for air circular rod of triangular lattice. The average dielectric constants for two cases increase as the filling factor or refractive index increase. Most field energies are localized in the high-dielectric

regions and consequently the normalized frequencies are reduced. For this reason, the overall photonic dispersion curves of either E- polarization or H-polarization modes in Fig. 3.15(a) and (b) tend to move toward lower frequencies.

The gap width of E-polarization mode drastically varies with filling factor than that with the refractive index. The E-polarization gap widths are strongly dependent on the filling factor. The air-band frequency for a given E-polarization band gap is very sensitive to an increase in filing factor, whereas the dielectric-band frequency is almost insensitive to that. The invariable dielectric band may reflect that field energies can be well-localized in the dielectric rods, and the changes of cross section area of rods can not affect the field distribution. However, the fraction of field energy inside the dielectric rods may increase as filling factor increase. The increased average dielectric constant leads to reduce the air-band frequency and approaches to dielectric-band frequency when filling factor is greater than 0.75. The difference in sensitivity of consecutive bands is responsible for the decrease of E-polarization gap width for large filling factor. Moreover, the results have shown that there only exists an H-polarization gap throughout the calculations and both polarization band gaps can not overlap by varying parameters, such as refractive index contrast and filling factor.

It is known the size and position of photonic band gap can be adjusted by the lattice type, lattice elements, refractive index contrast, filling factor and reductions of rotational and structural symmetries. The degenerate bands in the first Brillouin zone can be lift. Recently, it has been reported that the PBG width can remarkably increase by the use of anisotropy materials in the photonic crystal.[63-65] The anisotropic photonic crystal possesses the

anisotropic optical properties with extraordinary and ordinary refractive indices. The extraordinary axis is set to be parallel to the axis of the rod. The refractive index is n_e when the electric field vector in the E-polarization mode is parallel to the extraordinary axis, while the refractive index is n_0 when the electric field vector in the H-polarization mode is perpendicular to the extraordinary axis. Because the refractive indices for E and H-polarization modes are different, therefore, it provides an opportunity to control the E- and H- polarization gaps separately.

In this work, we use tellurium (Te) material in the photonic crystal to understand the effect of anisotropic optical property on the band structure. Tellurium rods, which posses the anisotropic optical properties with refractive indices $n_e = 6.2$ and $n_o = 4.8$ in the wavelength regime between 3.5 and 14 μm. The further optical features of anisotropic Te rods in the photonic crystal will be examined in detail. Figure 3.16 shows the gap map as a function of filling factor. Because the refractive index for E-polarization mode is larger than H-polarization mode, the frequencies of E-polarization bands are decreased markedly than that of H-polarization bands. Therefore, the anisotropic photonic crystal can overlap both modes and appear a sizeable complete PBG.

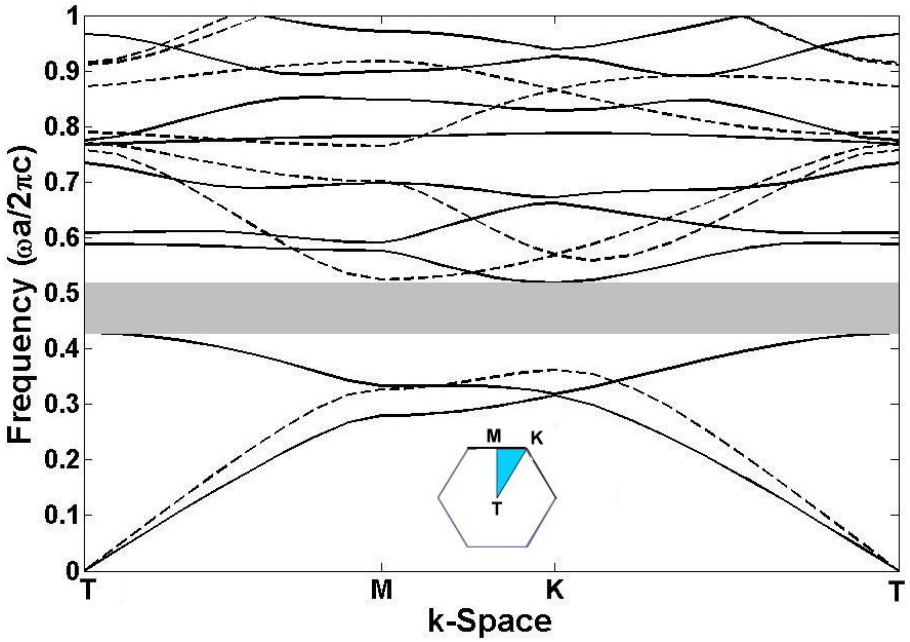

Figure 3.1 Photonic band structure of circular air rods in the triangular lattice, at a filling factor $f = 0.8$. The solid curves are for the E-polarization modes and the dotted curves are for the H-polarization modes.

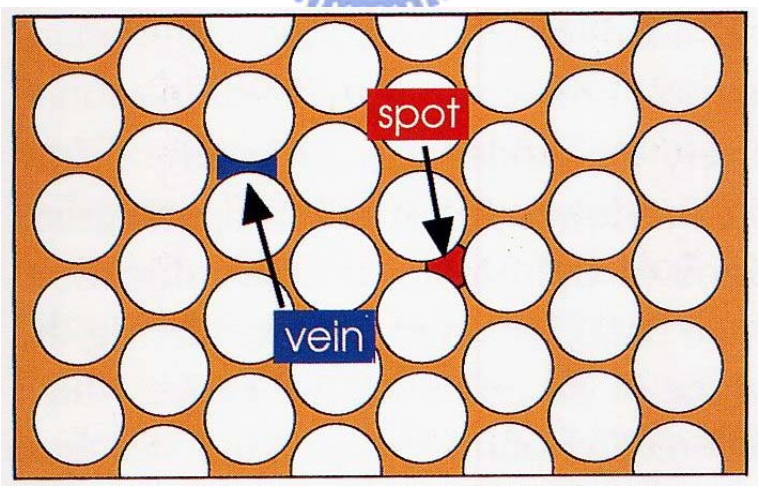

Figure 3.2 The schematic drawing of veins and spots in the triangular lattice. Between columns are narrow veins, connecting spots which are surrounded by three columns.

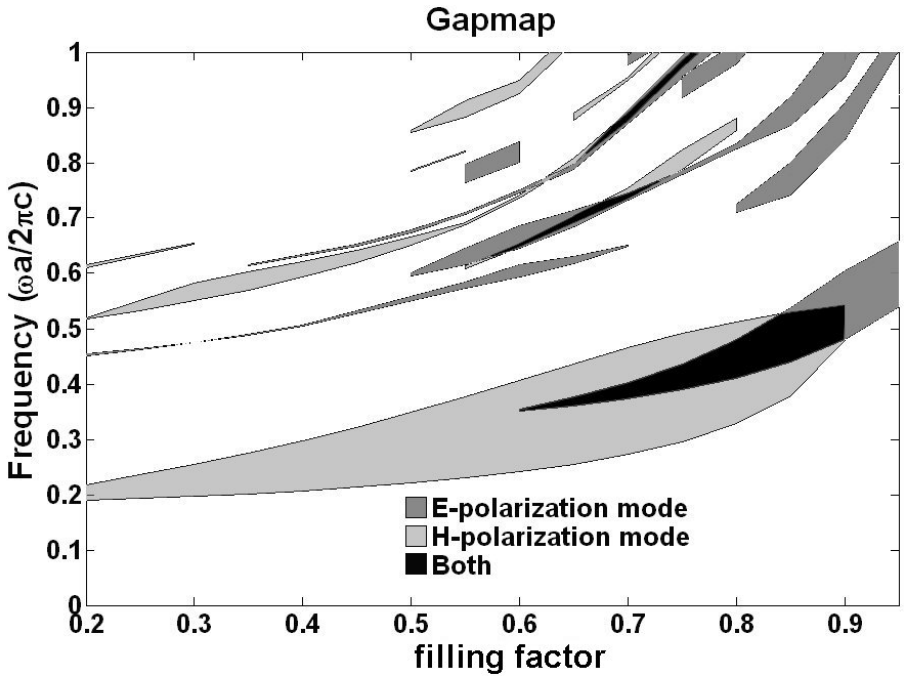

Figure 3.3 Gap widths as a function of filling factor of circular air rods in the triangular lattice.

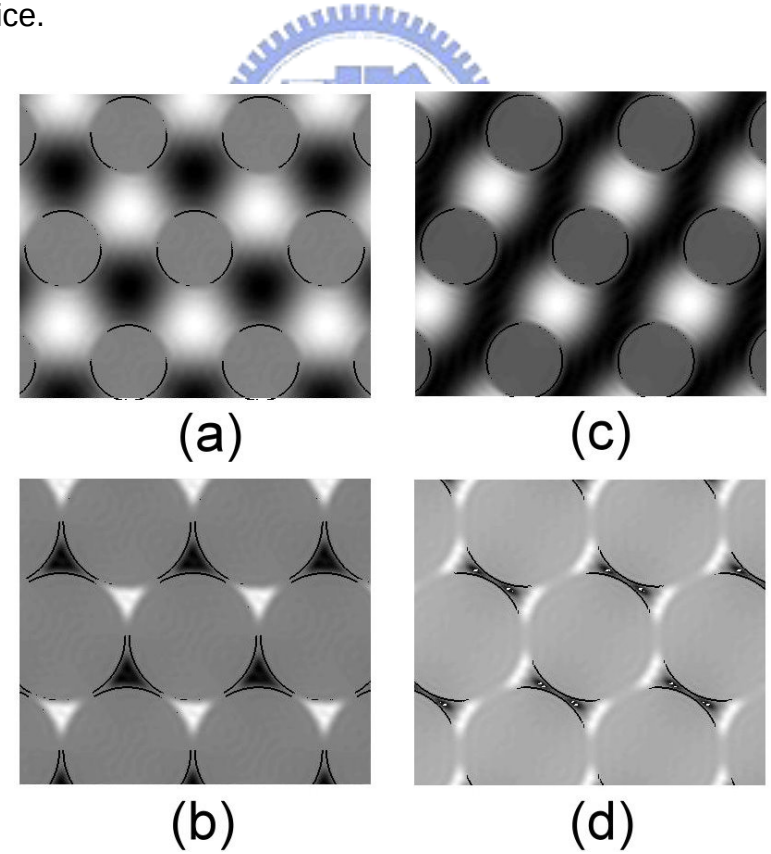

Figure 3.4 Displacement-field distribution of E-polarization modes associated with (a) first and (c) second bands at $f = 0.3$; (b) first and (d) second bands at $f = 0.85$. The fields are plotted at the T-symmetry point.

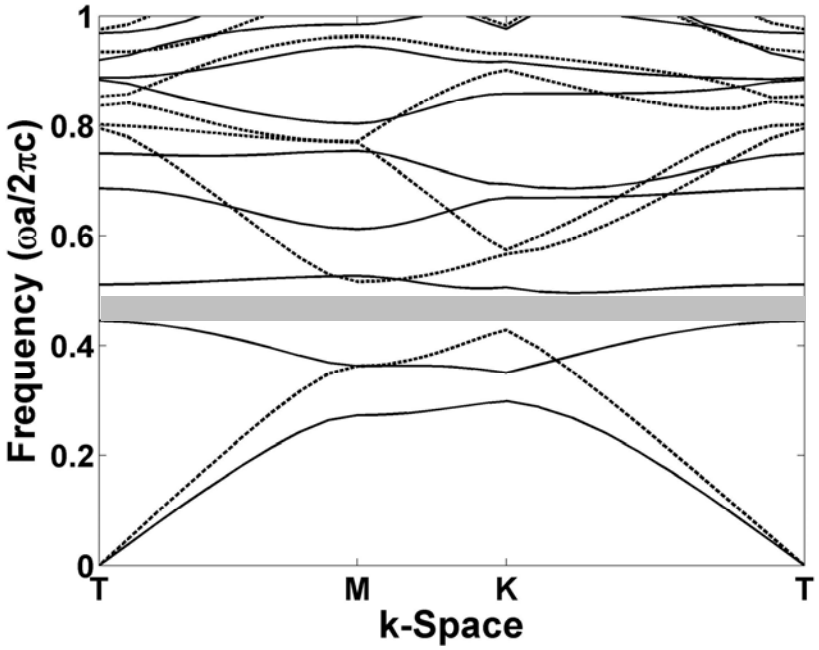

Figure 3.5 Photonic band structure of square air rods in the triangular lattice, at a filling factor $f = 0.8$.

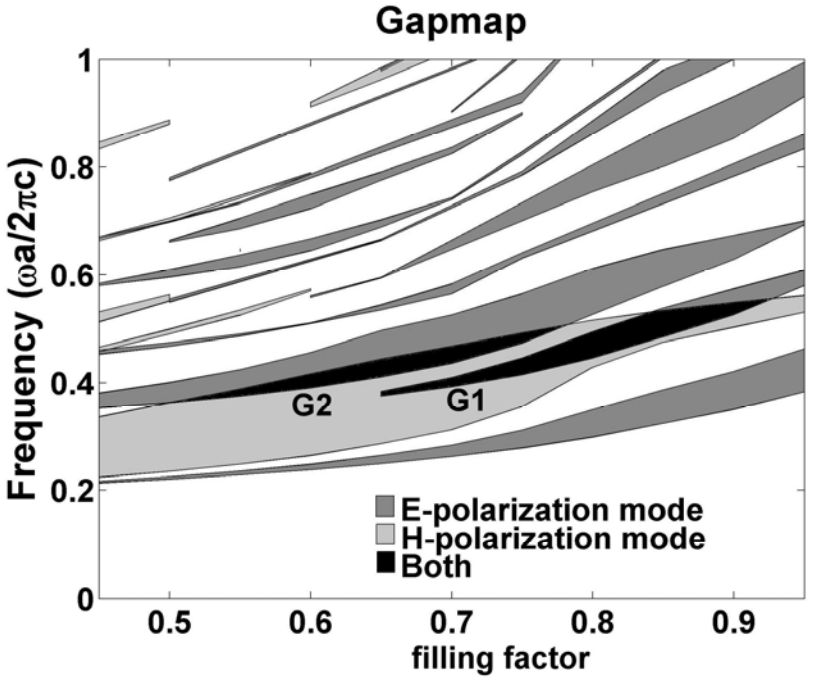

Figure 3.6 Gap widths as a function of filling factor of square air rods in the triangular lattice.

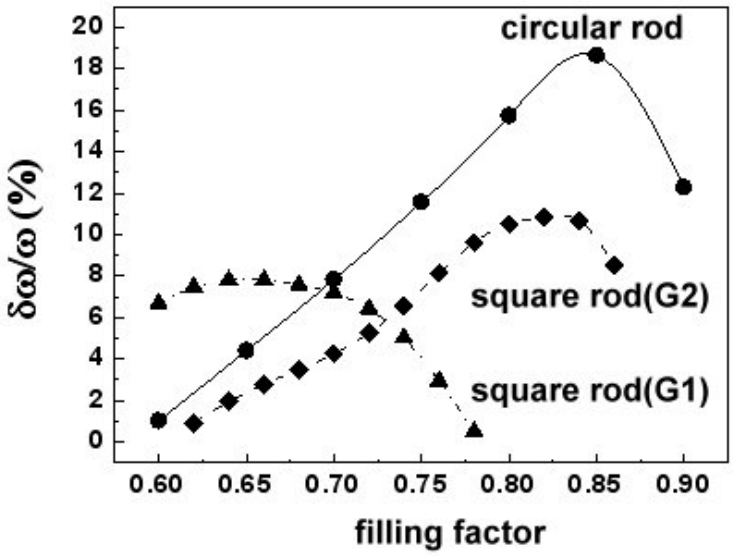

Figure 3.7 Complete gap widths to mid-gap frequency ratio as a function of filling factor for circular or square air rods in the triangular lattice.

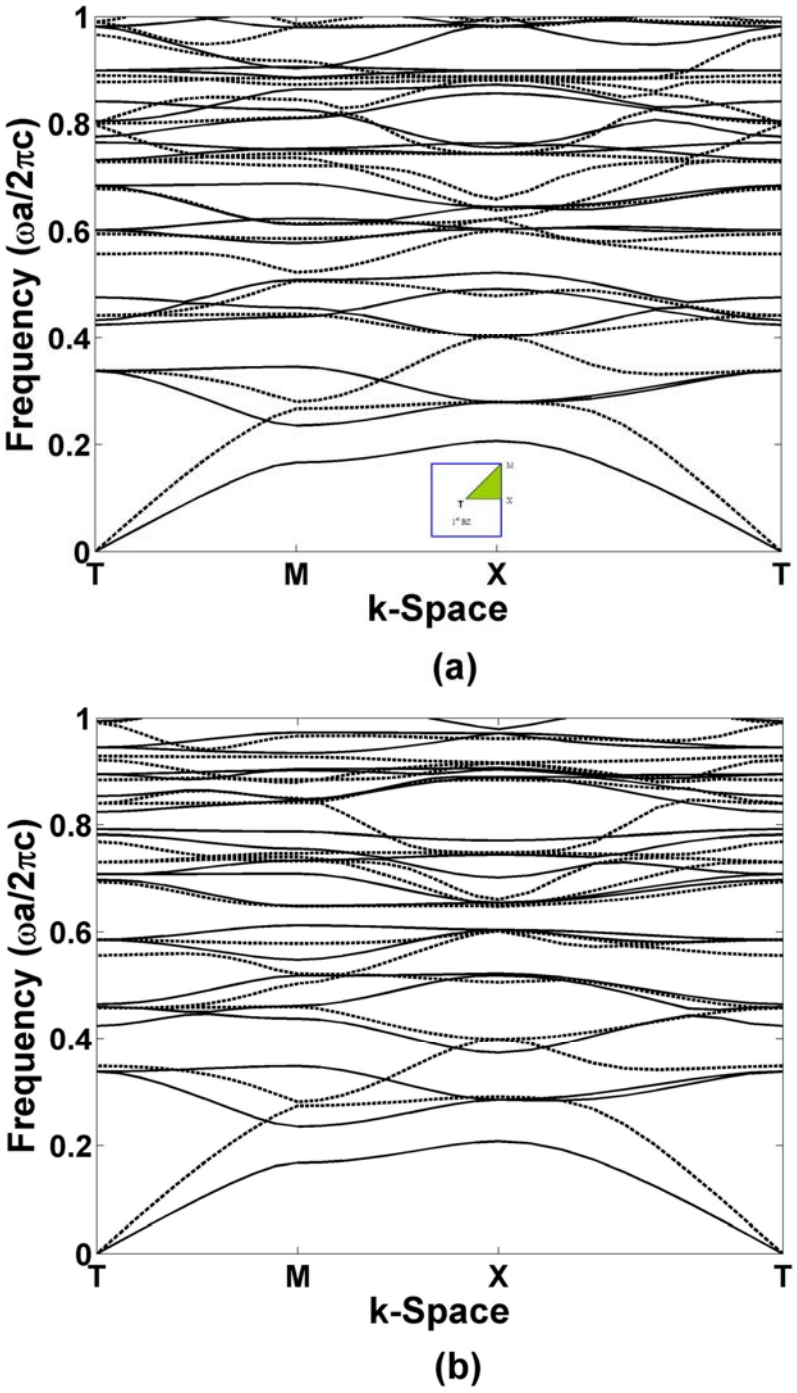

Figure 3.8 Photonic band structures associated with (a) circular and (b) square dielectric rods embedded with square lattice, at the filling factor of 0.45.

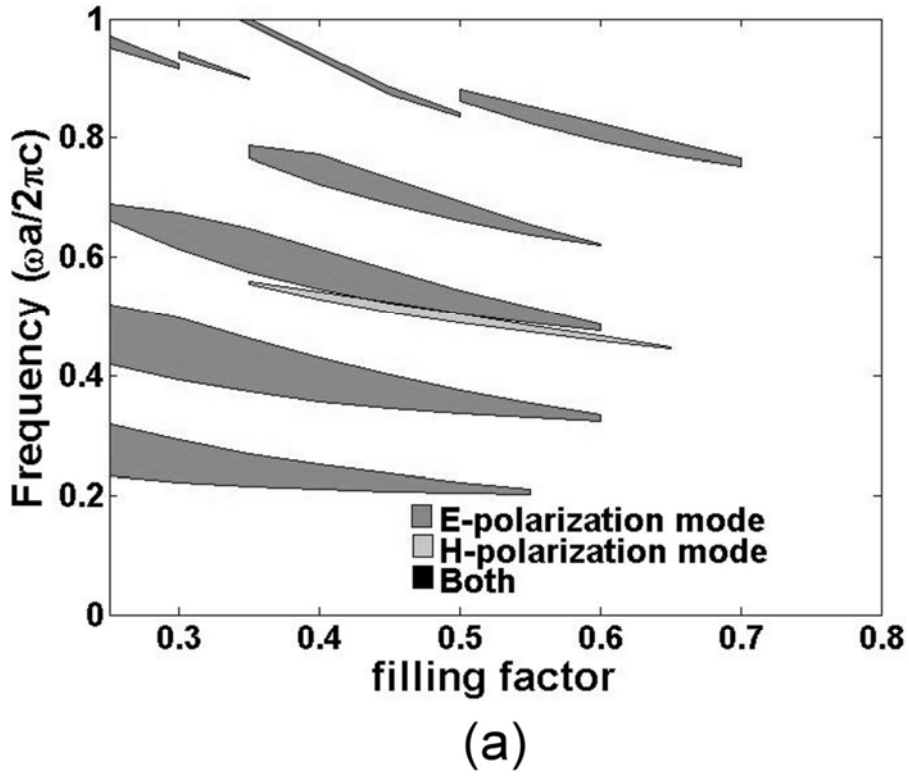

Figure 3.9 Gap map for the square lattice of (a) circular and (b) square dielectric rods as a function of filling factor.

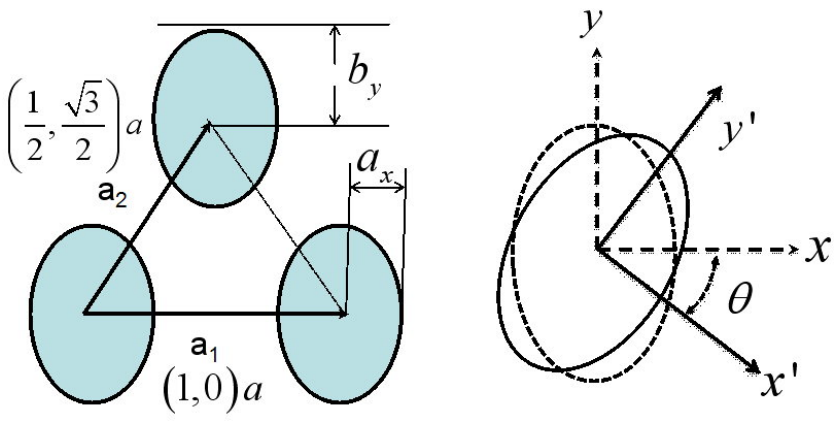

Figure 3.10 Schematic of oval rods in the triangular lattice. $\bar{a}_1$ and $\bar{a}_2$ are the basic vectors of the triangular lattice. a_x and b_y are the dimensions of major and minor axes. θ represents a rotating angle with respect to the x axis.

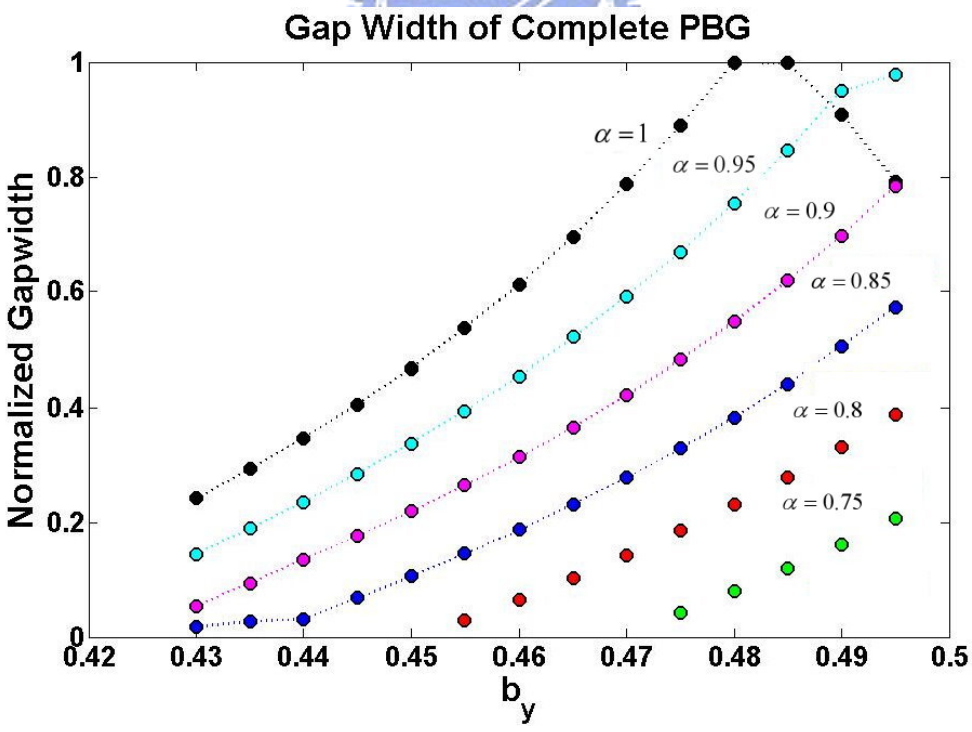

Figure 3.11 Normalized gap width of complete PBG as a function of b_y for various α.

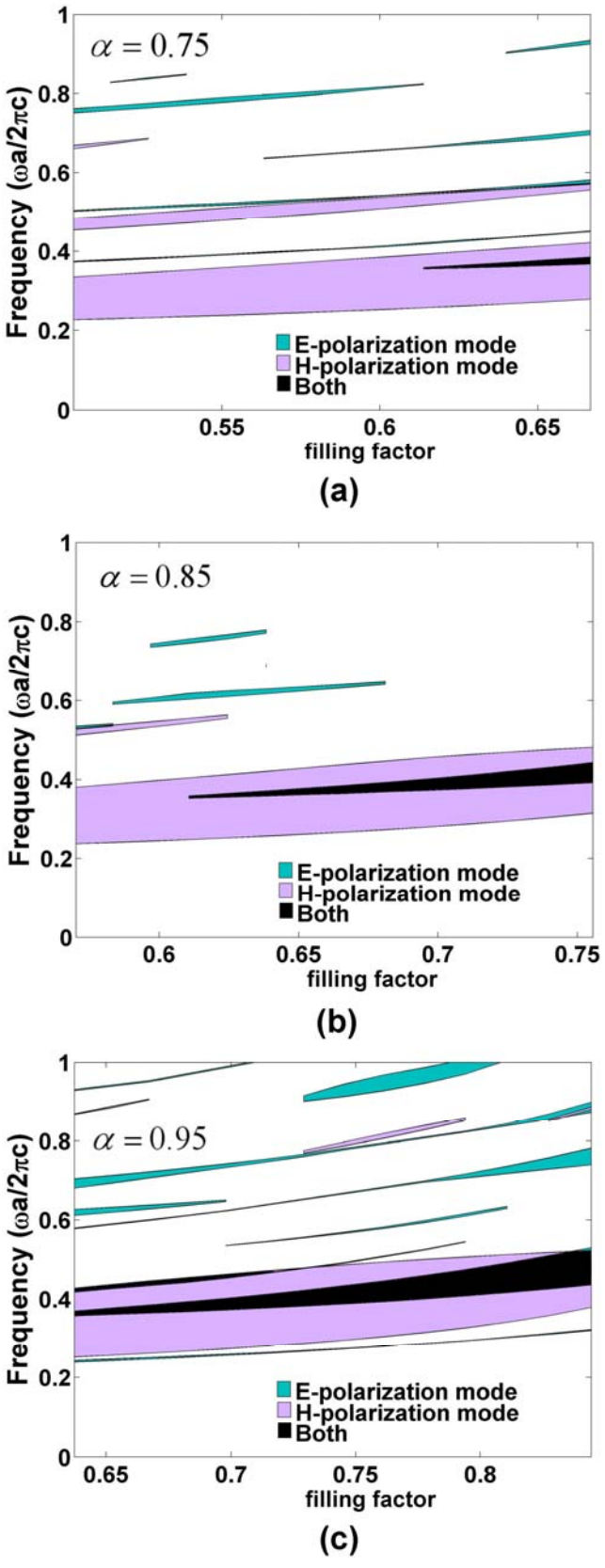

Figure 3.12 The dependence of gap map on filling factor of (a) $\alpha = 0.75$, (b) $\alpha = 0.85$ and (c) $\alpha = 0.95$.

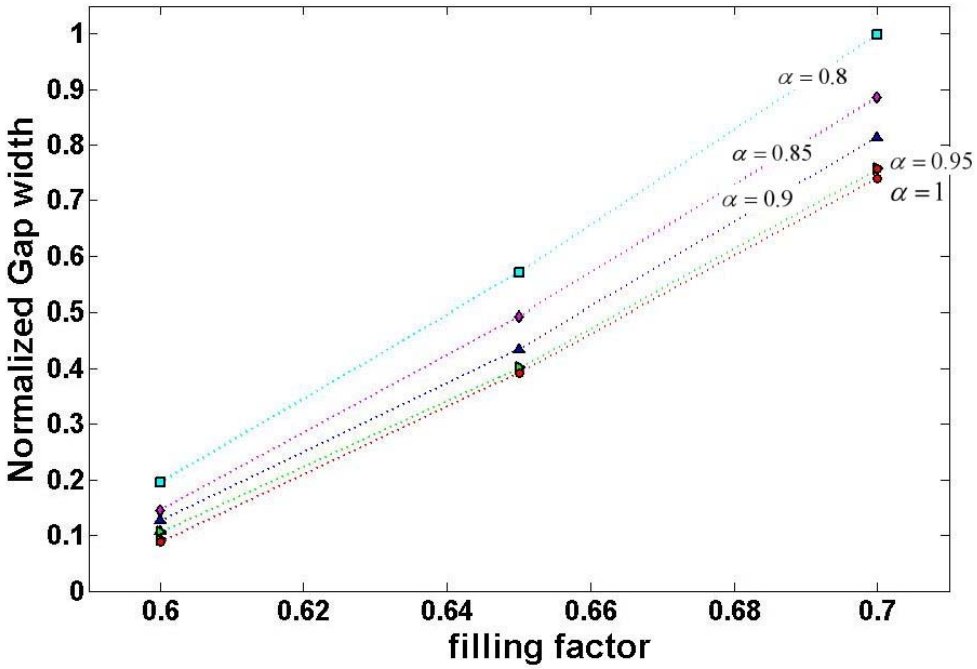

Figure 3.13 The dependence of normalized complete gap width on f for various α through a rotation angle of $\theta = 30^{\circ}$.

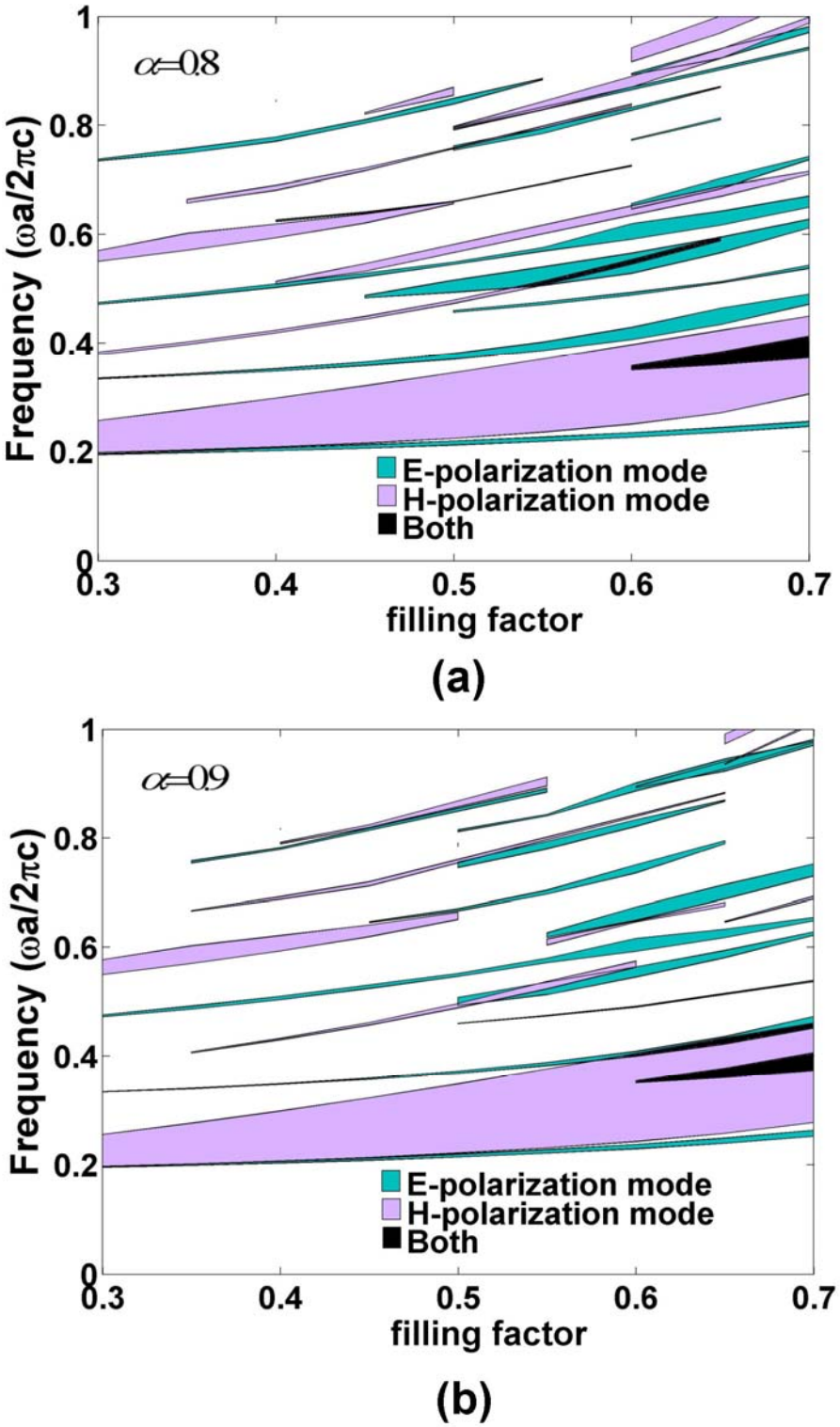

Figure 3.14 The dependence of gap map on filling factor of (a) $\alpha = 0.8$ and (b) $\alpha = 0.9$ through a rotation angle of $\theta = 30^{\circ}$.

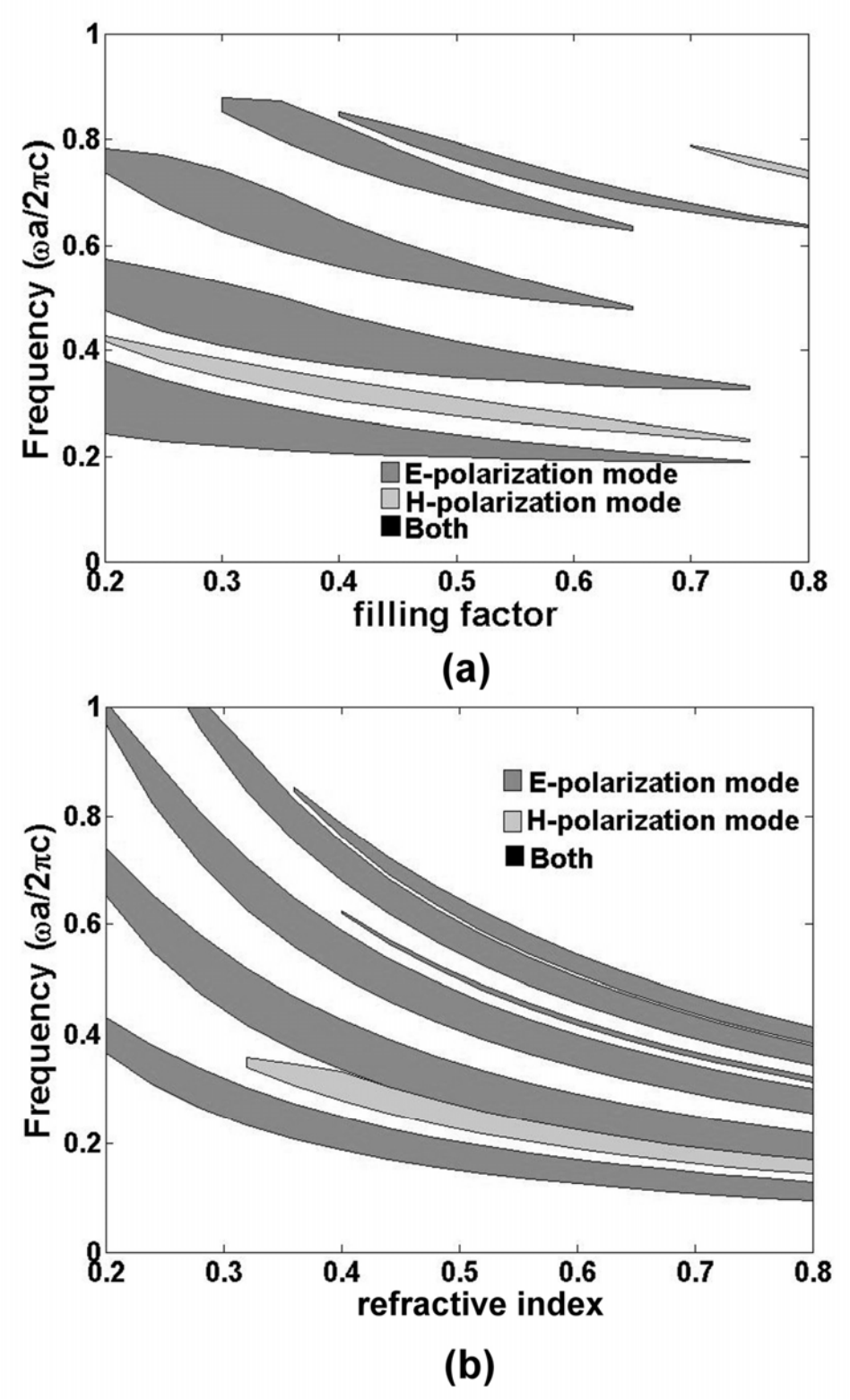

Figure 3.15 Gap maps plotted with respect to the (a) filling factor and (b) refractive index for circular dielectric rods in the triangular lattice.

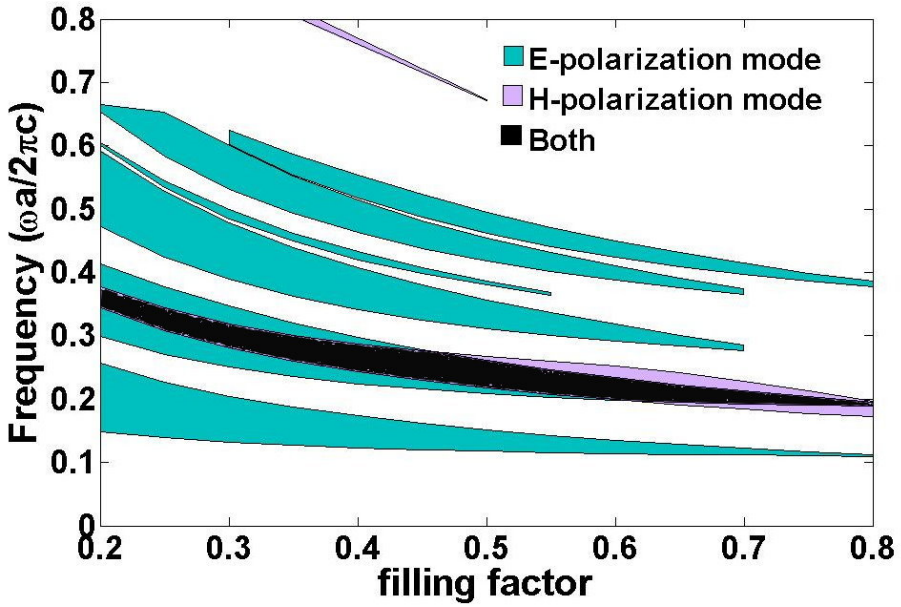

Figure 3.16 The gap map as a function of filling factor of circular anisotropic rods in the triangular lattice.